Habitable Exoplanet Imager Optical Telescope Concept Design

H. Philip Stahl,[a]

[a] NASA MARSHALL SPACE FLIGTH CENTER, HUNTSVILLE, AL 35812

ABSTRACT

The Habitable Exoplanet Imaging Mission (HabEx) is one of four missions under study for the 2020 Astrophysics Decadal Survey. Its goal is to directly image and spectroscopically characterize planetary systems in the habitable zone of Sun-like stars. Additionally, HabEx will perform a broad range of general astrophysics science enabled by 100 to 2500 nm spectral range and 3 x 3 arc-minute FOV. Critical to achieving the HabEx science goals is a large, ultra-stable UV/Optical/Near-IR (UVOIR) telescope. The baseline HabEx telescope is a 4-meter off-axis unobscured three-mirror-anastigmatic, diffraction limited at 400 nm with wavefront stability on the order of a few 10s of picometers. This paper summarizes the opto-mechanical design of the HabEx baseline optical telescope assembly, including a discussion of how science requirements drive the telescope's specifications, and presents analysis that the baseline telescope structure meets its specified tolerances.

Keywords: space telescopes, astrophysics, astronomy, HabEx

1. INTRODUCTION

"Are we alone in the Universe?" is probably the most compelling science question of our generation. Per the 2010 *New Worlds, New Horizons* Decadal Report[1]: "One of the fastest growing and most exciting fields in astrophysics is the study of planets beyond our solar system. The ultimate goal is to image rocky planets that lie in the habitable zone of nearby stars." The Survey recommended, as its highest priority, medium-scale activity such as a "New Worlds Technology Development (NWTD) Program" to "lay the technical and scientific foundations for a future space imaging and spectroscopy mission." The National Research Council (NRC) report, *NASA Space Technology Roadmaps & Prioroties*[2], states that the second highest technical challenge for NASA regarding expanding our understanding of Earth and the universe in which we live is to "Develop a new generation of astronomical telescopes that enable discovery of habitable planets, facilitate advances in solar physics, and enable the study of faint structures around bright objects by developing high-contrast imaging and spectroscopic technologies to provide unprecedented sensitivity, field of view, and spectroscopy of faint objects." As a result, NASA is studying in detail the Habitable Exoplanet Imaging Mission (HabEx) for the 2020 Decadal Survey.[3,4]

The goal of HabEx is to directly image planetary systems around Sun-like stars. And, while HabEx will be sensitive to all types of planets, its main goal is to directly image and characterize the atmospheres of Earth-like exoplanets in the Habitable Zone. By measuring the spectra of these planets, HabEx will search for signatures of habitability such as water, and be sensitive to gases in the atmosphere possibility indicative of biological activity, such as oxygen or ozone. In addition to the search for life, HabEx will enable a broad range of general astrophysics investigations, from studying the earliest epochs of the history of the Universe, to understanding the life cycle and deaths of the most massive stars.

The opto-mechanical design of any optical telescope assembly (OTA) is a complicated, iterative systems engineering exercise that starts with system level specifications and requires experience driven intuition backed by detailed analysis. Section 2 presents how the HabEx OTA specifications are derived from the HabEx science requirements. And, how the HabEx OTA specifications are primarily driven by requirements imposed by the coronagraph. Section 3 describes how the system level specifications are flown into opto-mechanical tolerances for rigid body motions. Section 4 provides an overview of the baseline opto-mechanical OTA design. A design whose initial concept is entirely based on experiential intuition. Finally, Section 5 summarizes detailed dynamic analysis of the baseline opto-mechanical design which shows that the design, using proven technology, can achieve the performance specifications necessary to perform HabEx science. The baseline 4-m off-axis HabEx opto-mechanical telescope design 'closes'.

Stahl, H. Philip, Habitable Exoplanet Imager Optical Telescope Concept Design, UV/Optical/IR Space Telescopes and Instruments, SPIE 10398-5, 2017.

2. OPTICAL TELESCOPE ASSEMBLY SPECIFICATIONS

The HabEx Optical Telescope Assembly (OTA) design (optical and structural) specifications are almost completely driven by the needs of exoplanet science using an internal coronagraph. To image exoplanets in the habitable zone close to their host star using a coronagraph requires a telescope/coronagraph 'system' that can produce a 10^{-10} 'dark hole' with as small of an inner working angle (IWA) as possible and as large of an irradiance throughput as possible. The smaller the IWA and the larger the throughput, the greater the number of habitable zones that can be searched – the greater the science 'yield'. IWA is the minimum angular distance (on the sky) where the 'dark hole' begins – the location when the coronagraph can block 10^{10} of the host stars light (Figure 1). The ability to achieve a small IWA depends upon the telescope's ability to produce a small stable point spread function (PSF) with a compact stable encircled energy (EE). The smaller the EE, the smaller the IWA. The remaining specifications are provided by the desire to perform wide-field general astrophysics. Table 1 summarizes the HabEx OTA specifications.

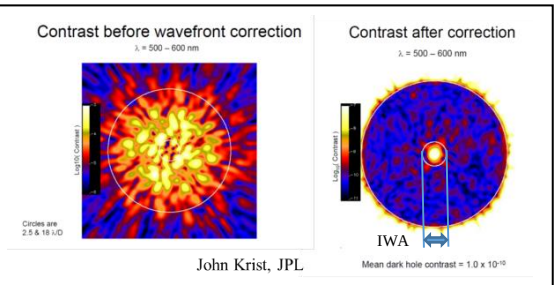

Figure 1: Exoplanet Dark Hole[5]

Table 1: HabEx Optical Telescope Specification			
Specification		Value	
Architecture		Off-Axis Unobscured Circular Aperture	
Optical Design		Three-Mirror Anastigmatic	
Science Instruments		Exo-C Configuration	
Aperture Diameter		> 4.0 meters	
Primary Mirror F/#		F/2.5 or slower	
Diffraction Limited Wavelength		400 nm	
Observatory WFE		< 35 nm rms	
OTA WFE		< 30 nm rms	
PMA SFE		< 8 nm rms	
	Low Spatial SFE (< 3 cycles/diameter)		< 5.6 nm rms
	Mid Spatial SFE (3 to 60 cycles/diameter)		< 5.6 nm rms
	High Spatial SFE (> 60 cycles/diameter)		< 0.6 nm rms
	Roughness		< 0.2 nm rms
Wavefront Error Stability		10 pm to 1 nm depending on coronagraph and spatial frequency	
Line of Sight Stability (Jitter)		< 0.5 milli-arc-seconds	

The IWA requirement drives two system specifications: aperture diameter and off-axis configuration. It is common knowledge that the larger a telescope's aperture, the smaller its point spread function (PSF) and its Encircled Energy (EE). But, what is often overlooked is that an unobscured (off-axis) telescope always has a more compact EE (better IWA) than an on-axis telescope with a central obscuration – because diffraction from the central obscuration broadens the PSF. To be specific, an unobscured circular aperture has 82.8% EE at λ/D; for a 10% central obscuration, 82.5% EE is at 1.4 λ/D; and, for a 20% obscuration, 82% EE is at 1.63 λ/D.[6] Thus to achieve similar IWA performance as an unobscured 4-m telescope, an on-axis telescope with 10% central obscuration would need to be at least 5.6-m and one with 20% obscuration would need to be at least 6.5-m. Additionally, diffraction from secondary mirror spider obscurations also distort the PSF and broaden the EE. A 1 to 2% wide spider can increase EE diameter (IWA) by 5 to 10%[6] – requiring a 5 to 10% larger on-axis telescope. Of course the problem is even worse for a segmented aperture primary mirror. Thus, the baseline HabEx optical telescope is an unobscured off-axis monolithic aperture configuration.

Because general astrophysics science desires a 3 x 3 arcminute field of view (FOV) for its imager and multi-object spectrograph, the HabEx is baselining a three mirror anastigmatic (TMA) design.

Regarding minimum aperture, based on a design reference mission yield estimate for an off-axis-telescope/coronagraph combination, the minimum desired aperture diameter is 4-meter.[7] And, while a larger aperture would provide higher yield, 4-m was selected as the baseline for several programmatic reasons. First, 4-m class mirrors are manufacturable. Schott has an existing infrastructure to melt and cast 4.2-m diameter by 42 cm thick Zerodur® mirror substrates. And, Corning has the infrastructure to either frit bond or low-temperature-fuse 4-m 'class' ULE® mirror substrates. And at least four organizations have existing infrastructure to grind and polish 4-m class substrates into space mirrors, including: United

Technology Optical Systems in Danbury CT, L3/Brashears in Pittsburgh, University of Arizona in Tucson and RESOC outside of Paris France. Second, a 4-m class telescope can be packaged inside of NASA's planned SLS 8.4-m fairing. Actually, the SLS can accommodate a larger telescope and HabEx plans to investigate potential 6-m class concepts.

Potentially the most important design parameter specification that significantly drives the opto-mechanical telescope design is the primary mirror's F/# or radius of curvature. From a packaging perspective, a fast PM F/# or short radius of curvature is desired. But, to minimize polarization cross-talk in the coronagraph, a slow PM F/# is desired. After consideration, it was decided to select an optical design similar to Exo-C with an F/2.5 primary mirror and the science instruments located on the anti-Sun side of the telescope.[8] This configuration minimizes the need for high incidence angle reflections that produce unwanted polarization effects and isolates the coronagraph of thermal disturbances. As a consequence, the HabEx OTA is physically long. For the baseline 4-m design, the separation between the primary and secondary mirrors is 9 meters. As points of reference, Hubble's PM is F/2.2 and Webb's PM is F/1.25.

Finally, the optical telescope wavefront error specification and primary mirror flow-down allocation are derived using standard methods. The specification is based on a desired 400 nm diffraction limited performance. The primary mirror allocation assumes computer controlled polishing for low spatial frequencies and a -2 slope for high spatial frequencies.

2.1 Wavefront Error Stability

Wavefront Error Stability is driven by the coronagraph. Any temporal or dynamic change in WFE can result in dark-hole speckles that produce a false exoplanet measurement or mask a true signal. The key issue is how large of a WFE can any given coronagraph tolerate. A leading candidate for HabEx is the Vector Vortex Coronagraph (VVC-N) where N indicates the 'charge' or azimuthal shear. The higher the 'charge' the more low order error it can tolerate, but the larger its inner working angle and lower its throughput. Thus, a VVC-4 is most desirable. Figure 2 summarizes specifications for the maximum amount of aberration which can be tolerated by VVC-4 to VVC-10.[9]

Aberration	Indices		Allowable RMS wavefront error (nm) per mode			
	n	m	charge 4	charge 6	charge 8	charge 10
Tip-tilt	1	±1	1.1	5.9	14	26
Defocus	2	0	0.8	4.6	12	26
Astigmatism	2	±2	0.0067	1.1	0.90	5
Coma	3	±1	0.0062	0.66	0.82	5
Spherical	4	0	0.0048	0.51	0.73	6
Trefoil	3	±3	0.0072	0.0063	0.57	0.67
2nd Astig.	4	±2	0.0080	0.0068	0.67	0.73
2nd Coma	5	±1	0.0036	0.0048	0.69	0.85
2nd Spher.	6	0	0.0025	0.0027	0.84	1
Quadrafoil	4	±4	0.0078	0.0080	0.0061	0.53
2nd Trefoil	5	±3	0.0051	0.0056	0.0043	0.72
3rd Astig.	6	±2	0.0023	0.0035	0.0034	0.81
3rd Coma	7	±1	0.0018	0.0022	0.0036	1.18
3rd Spher.	8	0	0.0018	0.0018	0.0033	1.49

Garreth Ruane, June 2017

not rejected
first-order rejection
> first-order rejection

Figure 2: Wavefront Stability Required by VVC

WFE instability arises from mechanical and thermal sources. Thermal errors occur when a telescope is slewed relative to the Sun. Thermal load changes cause the structure holding the mirrors to expand/contract (resulting in alignment drift) and the mirrors themselves to change shape. Fortunately, thermal effects are slow and can be corrected. The telescope design team assumes that any coronagraph will have a wavefront sensing and control (WFSC) capability – such that a sensor will quantify any change in WFE and command deformable mirrors (DMs) in the coronagraph to correct any change – to maintain the dark hole. The problem is that WFSC is not instantaneous. There is an update period, and the telescope must be stable at the required pm level for the duration of the update period. Depending upon the magnitude of the host star whose planetary system is being investigated, this update period may range from 10 to 20 to 30 minutes. To mitigate this issue, the telescope design team is baselining low coefficient of thermal expansion materials such as Zerodur® ceramic or Ultra-Low Expansion (ULE®) glass. Additionally, we are investigating the predictive thermal control technology to keep the telescope at a constant temperature.

Another source of WFE instability is mechanical disturbance. Mechanical forces (from reaction wheels, cryo-coolers, etc.) can excite inertial motion and vibrational modes in the mirrors and structure that holds them. Again, temporal frequency is important. WFIRST plans to have a low-order wavefront sensor (LOWFS) to sense and correct low-order errors. But, its bandwidth is only about 10 Hz. Preliminary analysis of the baseline HabEx opto-mechanical structure indicates that all rigid body modes causing WFE stability occur at frequencies above 25 Hz and are thus uncorrectable. However, there is one mitigating factor. While all mechanical vibration is in general bad, there are degrees of badness. If the motions are perfectly periodic, multiple cycles over an integration period will produce a symmetric pattern. If this pattern is 100% repeatable, it is possible to remove it through 'speckle subtraction'. But, if the vibration is not perfectly periodic, there will be a non-repeatable component to the error that cannot be calibrated and removed. Therefore, to be conservative, HabEx defines the tolerances summarized in Figure 2 to constitute the HabEx Wavefront Stability specification.

2.2 Line of Sight (LOS) Stability

LOD jitter is typically specified to be less than 1/10th the point spread function (PSF) radius. For a 400 nm diffraction limited 4-m telescope, the on-sky PSF radius is 25 mas. Thus, the jitter specification should be < 2.5 mas. But, coronagraphs require better LOS stability. The reason is that jitter causes beam shear on the secondary and tertiary mirrors, as well as other mirrors in the optical train. These beam shears introduce wavefront errors that result in contrast leakage.

The HabEx LOS stability specification[10] has three temporal regimes:

- Slow pointing drift (thermal) during an integration period shall be < 1 mas rms per axis
- Slow pointing jitter that can be corrected by a fine/fast steering mirror shall be < 1 mas rms per axis
- Fast pointing jitter that cannot be corrected by a fine/fast steering mirror shall be < 0.5 mas per axis

Please note that these LOS stability specifications depend on the exact optical prescriptions of all mirrors in the optical train and their fabrication quality, i.e. residual low-order and mid-spatial frequency errors.

To be conservative, for the purpose of designing the HabEx telescope opto-mechanical structure, the telescope design team is assuming that the telescope must have a LOS stability that meets the 'fast jitter' requirement. Preliminary design analysis indicates that all HabEx rigid body modes affecting LOS jitter occur at frequencies above 25 Hz. Thus, all telescope jitter is uncorrectable by either the spacecraft's attitude control system (which on WFIRST has a bandwidth of 0.05 Hz) or a low-order wavefront sensor (WFIRST's LOWFS has a bandwidth of approximately 10 Hz).[10] Thus, the 'on-sky' LOS Stability specification for the HabEx optical telescope assembly is < 0.5 mas. And, for the current HabEx optical design with its 80X magnification, the LOS Stability specification at the FSM is < 40 mas.

3. OPTICAL DESIGN TOLERANCE SENSITIVITY

To achieve the Wavefront (WFE) Stability and Line of Sight (LOS) Stability specifications requires an ultra-stable opto-mechanical telescope structure that can align the primary, secondary and tertiary mirrors to each other and maintain that alignment. Rigid body motions of the primary, secondary and tertiary mirrors introduce WFE and LOS errors. For example, a despace between the PM and SM introduces defocus, Y-coma, X-astig, spherical and Y-trefoil. A decenter between the PM and SM introduces astigmatism and defocus; and, LOS tilt. The exact amounts of each is calculated using ZEMAX tolerance analysis and presented in Sections 3.1 and 3.2. Table 2 provides potential rigid body specifications for the 4-meter off-axis F/2.5 baseline optical design to achieve the required WFE Stability for the VVC-4 WFE, VVC-6 WFE, and 0.5 mas LOS specification. Given the similarity of the specification for the VVC-4 and 0.5 mas LOS, one might argue that the VVC-4 should be the baseline instrument. The two most important DOFs are the primary mirror X- and Y-decenter and have been allocated the largest tolerance possible. Conversely, the tertiary mirror motions have very little effect on WFE stability and have been allocated tolerances deemed easily achieved.

Table 2. HabEx Optical Component Rigid Body Stability Tolerance Specification

Alignment	for VVC-4	for 0.5 mas LOS	for VVC-6	Units
PM X-Decenter	**4**	**15**	400	nanometers
PM Y-Decenter	**4**	**15**	400	nanometers
PM Z-Despace	8	8	500	nanometers
PM X-Tilt (Y-Rotation)	0.25	0.25	5	nano-radians
PM Y-Tilt (X-Rotation)	0.25	0.25	5	nano-radians
PM Z-Rotation	0.5	0.5	5	nano-radians
SM X-Decenter	4	4	400	nanometers
SM Y-Decenter	4	4	400	nanometers
SM Z-Despace	8	8	500	nanometers
SM X-Tilt (Y-Rotation)	0.5	0.5	5	nano-radians
SM Y-Tilt (X-Rotation)	0.5	0.5	5	nano-radians
SM Z-Rotation	0.5	0.5	5	nano-radians
TM X-Decenter	10	10	1000	nanometers
TM Y-Decenter	10	10	1000	nanometers
TM Z-Despace	1000	1000	1000	nanometers
TM X-Tilt (Y-Rotation)	10	10	1000	nano-radians
TM Y-Tilt (X-Rotation)	10	10	1000	nano-radians
TM Z-Rotation	1000	1000	1000	nano-radians

3.1 Optical Design Sensitivity to Line of Sight Stability

A Zemax tolerance analysis provides the LOS sensitivity to rigid body motions of the primary, secondary and tertiary mirror alignment for the baseline F/2.5 optical design (Table 3).[11]

Table 3. LOS Sensitivity to Component Rigid Body Alignment

Alignment	ZEMAX	Tolerance	Units	X-Tilt	Y-Tilt	Units
PM X-Decenter	DX	1	nm	1.72	0	mas
PM Y-Decenter	DY	1	nm	0	1.67	mas
PM Z-Despace	DZ	1	nm	0	0.43	mas
PM X-Tilt (Y-Rotation)	TY	1	mas	-165.31	0	mas
PM Y-Tilt (X-Rotation)	TX	1	mas	0	167.98	mas
PM Z-Rotation	TZ	1	mas	20.88	0	mas
SM X-Decenter	DX	1	nm	-1.53	0	mas
SM Y-Decenter	DY	1	nm	0	-1.48	mas
SM Z-Despace	DZ	1	nm	0	-0.43	mas
SM X-Tilt (Y-Rotation)	TY	1	mas	14.54	0	mas
SM Y-Tilt (X-Rotation)	TX	1	mas	0	-14.8	mas
SM Z-Rotation	TZ	1	mas	-1.62	0	mas
TM X-Decenter	DX	1	nm	-0.19	0	mas
TM Y-Decenter	DY	1	nm	0	-.019	mas
TM Z-Despace	DZ	1	nm	0	0	mas
TM X-Tilt (Y-Rotation)	TY	1	mas	2.02	0	mas
TM Y-Tilt (X-Rotation)	TX	1	mas	0	-2.02	mas
TM Z-Rotation	TZ	1	mas	0.0036	0	mas

Note that Zemax uses linear displacement units of nanometers and angular rotation units of milli-arc-seconds. And, the LOS X- and Y-Tilt error is also in units of milli-arc-seconds. The tolerance analysis converts these to n-radians.

Using the alignment LOS sensitivity analysis of Table 3, an excel spreadsheet was created to evaluate different alignment allocations to achieve the LOS stability specification (Figure 3). The spreadsheet calculates the LOS error for each rigid body degree of freedom (DOF) then calculates the RSS of each DOF. Given, as discussed in Section 5, that the two rigid body motion response modes that have the highest impact on LOS stability are the 25 Hz Primary Mirror X- and Y-decenter modes, as much tolerance as possible is allocated to these modes.

LOS RSS Error										40.00	mas
					Sensitivity at FSM			ERROR		ALLOCATION (one sided P	
Alignment	ZEMAX	Tolerance	units	Input	Units	Y-Tilt	X-Tilt	Y-Tilt	X-Tilt	RSS	Units
PM X-Decenter	DX	15	nanometer	1	nanometer	1.72	0	25.80	0.00	25.80	mas
PM Y-Decenter	DY	15	nanometer	1	nanometer	0	1.67	0.00	25.05	25.05	mas
PM Z-Despace	DZ	8	nanometer	1	nanometer	0	0.43	0.00	3.44	3.44	mas
PM Y-Tilt	TX	0.25	nano-radian	1	mas	0	167.98	0.00	8.66	8.66	mas
PM X-Tilt	TY	0.25	nano-radian	1	mas	-165.31	0	-8.52	0.00	8.52	mas
PM Z-Rotation	TZ	0.5	nano-radian	1	mas	20.88	0	2.15	0.00	2.15	mas
SM X-Decenter	DX	4	nanometer	1	nanometer	-1.53	0	-6.12	0.00	6.12	mas
SM Y-Decenter	DY	4	nanometer	1	nanometer	0	-1.48	0.00	-5.92	5.92	mas
SM Z-Despace	DZ	8	nanometer	1	nanometer	0	-0.43	0.00	-3.44	3.44	mas
SM Y-Tilt	TX	0.5	nano-radian	1	mas	0	-14.8	0.00	-1.53	1.53	mas
SM X-Tilt	TY	0.5	nano-radian	1	mas	14.54	0	1.50	0.00	1.50	mas
SM Z-Rotation	TZ	0.5	nano-radian	1	mas	-1.62	0	-0.17	0.00	0.17	mas
TM X-Decenter	DX	10	nanometer	1	nanometer	-0.19	0	-1.90	0.00	1.90	mas
TM Y-Decenter	DY	10	nanometer	1	nanometer	0	-0.19	0.00	-1.90	1.90	mas
TM Z-Despace	DZ	1000	nanometer	1	nanometer	0	0	0.00	0.00	0.00	mas
TM Y-Tilt	TX	10	nano-radian	1	mas	0	-2.02	0.00	-4.17	4.17	mas
TM X-Tilt	TY	10	nano-radian	1	mas	2.02	0	4.17	0.00	4.17	mas
TM Z-Rotation	TZ	1000	nano-radian	1	mas	0.0036	0	0.74	0.00	0.74	mas
							SUM	17.65	20.20	105.18	mas
							RSS	28.36	28.01	39.86	mas

Figure 3: A potential rigid body motion tolerance allocation to produce 40 mas of line of sight stability at the fine/fast steering mirror when exposed to the JWST vibration specification with JWST vibration isolation.

3.2 Optical Design Sensitivity to Wavefront Error Stability

Figure 4 shows the Zemax tolerance analysis WFE (decomposed into RMS Zernike Coefficients) sensitivity to rigid body motions of the Primary, Secondary and Tertiary mirror alignment for the baseline F/2.5 optical design.[12] In Zemax notation (DX, DY, DZ) are lateral displacements of the mirror along its local coordinates and (TX, TY, TZ) are rotations or the mirror about its local coordinates. The total wavefront error introduced by each rigid body degree of freedom is decomposed into RMS Zernike Coefficients. Please note that Zemax does NOT adhere to the ISO standard regarding Zernike Coefficient Ordering and that the Zemax output was be reordered for subsequent analysis. It should also be noted that the tertiary mirror contributes very little WFE. And, no terms above 2 astigmatism contribute any WFE.

	Primary Mirror or M1						Secondary Mirror or M2						Tertiary Mirror or M3					
	DX	DY	DZ	TX	TY	TZ	DX	DY	DZ	TX	TY	TZ	DX	DY	DZ	TX	TY	TZ
	micron	micron	micron	arc-sec	arc-sec	arc-sec	micron	micron	micron	arc-sec	arc-sec	arc-sec	micron	micron	micron	arc-sec	arc-sec	arc-sec
	1	1	1	0.1	0.10	0.1	1	1	1	0.1	0.1	0.1	1	1	1	0.1	0.1	0.1
	nm	nm	nm	n-rad	n-rad	n-rad	nm	nm	nm	n-rad	n-rad	n-rad	nm	nm	nm	n-rad	n-rad	n-rad
	1000	1000	1000	484.81	484.81	484.81	1000	1000	1000	484.81	484.81	484.81	1000	1000	1000	484.81	484.81	484.81
Piston	-0.000004	-0.009726	0.076058	0.000020	0.000002	-0.000001	-0.000115	0.009713	-0.077023	-0.000004	-0.000119	-0.000003	0.000297	0.000034	0.120700	0.000001	-0.000327	-0.000885
X-Tilt	0.002597	0.000000	0.000001	0.000000	-0.001581	0.000812	-0.002593	0.000000	-0.000004	0.000000	0.000282	-0.000071	-0.000008	0.000000	0.000435	0.000000	0.000009	0.000024
Y-Tilt	0.000004	0.002356	0.002554	0.001635	-0.000003	0.000001	-0.000004	-0.002352	-0.002555	-0.000291	0.000000	0.000000	0.000000	-0.000009	0.000047	-0.000010	0.000000	0.000000
Defocus	-0.000002	-0.005585	0.043749	0.000017	0.000002	-0.000001	-0.000066	0.005577	-0.044306	-0.000003	-0.000069	-0.000002	0.000171	0.000019	0.069642	0.000001	-0.000188	-0.000511
Y-Astig	-0.004010	-0.000043	-0.000001	-0.000053	0.002441	-0.001254	0.004005	0.000038	0.000006	0.000070	-0.000435	0.000110	0.000013	0.000013	-0.000666	-0.000105	-0.000014	-0.000037
X-Astig	-0.000042	0.003889	0.001980	0.002525	0.000053	-0.000013	0.000037	-0.003883	-0.001981	-0.000450	-0.000070	0.000001	0.000014	-0.000014	0.000071	-0.000015	0.000105	-0.000040
Y-Coma	0.000001	0.000829	0.000896	0.000575	-0.000001	0.000000	-0.000001	-0.000828	-0.000897	-0.000102	0.000000	0.000000	0.000000	-0.000003	0.000016	-0.000004	0.000000	0.000000
X-Coma	0.000913	0.000000	0.000000	0.000000	-0.000556	0.000286	-0.000912	0.000000	-0.000002	0.000000	0.000099	-0.000025	-0.000003	0.000000	0.000154	0.000000	0.000003	0.000009
Y-Trefoil	0.000000	0.000042	0.000021	0.000027	0.000000	0.000000	0.000000	-0.000042	-0.000021	-0.000005	0.000000	0.000000	0.000000	0.000000	0.000000	0.000000	0.000000	0.000000
X-Trefoil	0.000043	0.000000	0.000000	0.000000	-0.000026	0.000014	-0.000043	0.000000	0.000000	0.000000	0.000005	-0.000001	0.000000	0.000000	0.000001	0.000000	0.000000	0.000000
Spherical	0.000000	0.000023	-0.000126	0.000004	0.000000	0.000000	0.000000	-0.000023	0.000126	-0.000001	0.000000	0.000000	0.000000	0.000000	-0.000034	0.000000	0.000000	0.000000
2 astig	0.000000	-0.000016	-0.000012	-0.000010	0.000000	0.000000	0.000000	0.000016	0.000012	0.000002	0.000000	0.000000	0.000000	0.000000	0.000000	0.000000	0.000000	0.000000
2 astig	0.000017	0.000000	0.000000	0.000000	-0.000010	0.000005	-0.000017	0.000000	0.000000	0.000000	0.000002	0.000000	0.000000	0.000000	0.000000	0.000000	0.000000	0.000000
Quadrafoil	0.000000	0.000000	0.000000	0.000000	0.000000	0.000000	0.000000	0.000000	0.000000	0.000000	0.000000	0.000000	0.000000	0.000000	0.000000	0.000000	0.000000	0.000000
Quadrafoil	0.000000	0.000000	0.000000	0.000000	0.000000	0.000000	0.000000	0.000000	0.000000	0.000000	0.000000	0.000000	0.000000	0.000000	0.000000	0.000000	0.000000	0.000000
2 coma	-0.000003	0.000000	0.000000	0.000000	0.000002	-0.000001	0.000003	0.000000	0.000000	0.000000	0.000000	0.000000	0.000000	0.000000	0.000000	0.000000	0.000000	0.000000
2 coma	0.000000	-0.000002	-0.000004	-0.000002	0.000000	0.000000	0.000000	0.000002	0.000004	0.000000	0.000000	0.000000	0.000000	0.000000	0.000000	0.000000	0.000000	0.000000
2 trefoil	0.000000	0.000000	0.000000	0.000000	0.000000	0.000000	0.000000	0.000000	0.000000	0.000000	0.000000	0.000000	0.000000	0.000000	0.000000	0.000000	0.000000	0.000000
2 trefoil	0.000000	0.000000	0.000000	0.000000	0.000000	0.000000	0.000000	0.000000	0.000000	0.000000	0.000000	0.000000	0.000000	0.000000	0.000000	0.000000	0.000000	0.000000
Pentafoil	0.000000	0.000000	0.000000	0.000000	0.000000	0.000000	0.000000	0.000000	0.000000	0.000000	0.000000	0.000000	0.000000	0.000000	0.000000	0.000000	0.000000	0.000000
Pentafoil	0.000000	0.000000	0.000000	0.000000	0.000000	0.000000	0.000000	0.000000	0.000000	0.000000	0.000000	0.000000	0.000000	0.000000	0.000000	0.000000	0.000000	0.000000

Figure 4: HabEx baseline 4-m off-axis F/2.5 optical design WFE Stability decomposed into RMS Zernikes.

An excel spreadsheet (Figure 5) evaluates different alignment allocations to achieve the required WFE stability required for the VVC. The spreadsheet calculates the RMS Zernike Coefficient for each rigid body degree of freedom (DOF) then RSS these coefficients based upon the DOF allocation to obtain a total RMS Zernike WFE in nanometers.

			Primary Mirror or M1						Secondary Mirror or M2						Tertiary Mirror or M3					
			DX	DY	DZ	TX	TY	TZ	DX	DY	DZ	TX	TY	TZ	DX	DY	DZ	TX	TY	TZ
			X-Decenter	Y-Decenter	Z-Despace	Y-Tilt	X-Tilt	Z-Rotation	X-Decenter	Y-Decenter	Z-Despace	Y-Tilt	X-Tilt	Z-Rotation	X-Decenter	Y-Decenter	Z-Despace	Y-Tilt	X-Tilt	Z-Rotation
			nm	nm	nm	n-rad	n-rad	n-rad	nm	nm	nm	n-rad	n-rad	n-rad	nm	nm	nm	n-rad	n-rad	n-rad
INPUT DOF SPECIFICATION			**4.00**	**4.00**	8.00	0.25	0.25	0.50	4.00	4.00	8.00	0.50	0.50	0.50	10.00	10.00	1000.00	10.00	10.00	1000.00
	VVC4 TOLERANCE	WFE																		
ISO RMS Zernikes	nm	nm																		
Z0 Piston			0.000	-0.010	0.076	0.000	0.000	0.000	0.000	0.010	-0.077	0.000	0.000	0.000	0.000	0.000	0.121	0.000	0.000	-0.001
Z1 X-Tilt	1.1	0.0041	0.003	0.000	0.000	0.000	-0.002	0.001	-0.003	0.000	0.000	0.000	0.000	0.000	0.000	0.000	0.000	0.000	0.000	0.000
Z2 Y-Tilt	1.1	0.0052	0.000	0.002	0.003	0.002	0.000	0.000	0.000	-0.002	-0.003	0.000	0.000	0.000	0.000	0.000	0.000	0.000	0.000	0.000
Z3 Focus	0.8	0.0938	0.000	-0.006	0.044	0.000	0.000	0.000	0.000	0.006	-0.044	0.000	0.000	0.000	0.000	0.000	0.070	0.000	0.000	-0.001
Z4 X-Astig	0.0067	0.0067	0.000	0.004	0.002	0.003	0.000	0.000	0.000	-0.004	-0.002	0.000	0.000	0.000	0.000	0.000	0.000	0.000	0.000	0.000
Z5 Y-Astig	0.0067	0.0063	-0.004	0.000	0.000	0.000	0.002	-0.001	0.004	0.000	0.000	0.000	0.000	0.000	0.000	0.000	-0.001	0.000	0.000	0.000
Z6 X-Coma	0.0062	0.0014	0.001	0.000	0.000	0.000	-0.001	0.000	-0.001	0.000	0.000	0.000	0.000	0.000	0.000	0.000	0.000	0.000	0.000	0.000
Z7 Y-Coma	0.0062	0.0018	0.000	0.001	0.001	0.001	0.000	0.000	0.000	-0.001	-0.001	0.000	0.000	0.000	0.000	0.000	0.000	0.000	0.000	0.000
Z8 Sphere	0.0048	0.0002	0.000	0.000	0.000	0.000	0.000	0.000	0.000	0.000	0.000	0.000	0.000	0.000	0.000	0.000	0.000	0.000	0.000	0.000
Z9 X-Trefoil	0.0072	0.0001	0.000	0.000	0.000	0.000	0.000	0.000	0.000	0.000	0.000	0.000	0.000	0.000	0.000	0.000	0.000	0.000	0.000	0.000
Z10 Y-Trefoil	0.0072	0.0001	0.000	0.000	0.000	0.000	0.000	0.000	0.000	0.000	0.000	0.000	0.000	0.000	0.000	0.000	0.000	0.000	0.000	0.000
Z11 X-2nd Astig	0.008	0.0000	0.000	0.000	0.000	0.000	0.000	0.000	0.000	0.000	0.000	0.000	0.000	0.000	0.000	0.000	0.000	0.000	0.000	0.000
Z12 Y-2nd Astig	0.008	0.0000	0.000	0.000	0.000	0.000	0.000	0.000	0.000	0.000	0.000	0.000	0.000	0.000	0.000	0.000	0.000	0.000	0.000	0.000
Z13 X-2nd Coma	0.0036	0.0000	0.000	0.000	0.000	0.000	0.000	0.000	0.000	0.000	0.000	0.000	0.000	0.000	0.000	0.000	0.000	0.000	0.000	0.000
Z14 Y-2nd Coma	0.0036	0.0000	0.000	0.000	0.000	0.000	0.000	0.000	0.000	0.000	0.000	0.000	0.000	0.000	0.000	0.000	0.000	0.000	0.000	0.000
Z15 2nd Sphere	0.0025	0.0000	0.000	0.000	0.000	0.000	0.000	0.000	0.000	0.000	0.000	0.000	0.000	0.000	0.000	0.000	0.000	0.000	0.000	0.000
Z16 X-Quadrafoil	0.0078	0.0000	0.000	0.000	0.000	0.000	0.000	0.000	0.000	0.000	0.000	0.000	0.000	0.000	0.000	0.000	0.000	0.000	0.000	0.000
Z17 Y-Quadrafoil	0.0078	0.0000	0.000	0.000	0.000	0.000	0.000	0.000	0.000	0.000	0.000	0.000	0.000	0.000	0.000	0.000	0.000	0.000	0.000	0.000
Z18 X-2nd Trefoil	0.0051	0.0000	0.000	0.000	0.000	0.000	0.000	0.000	0.000	0.000	0.000	0.000	0.000	0.000	0.000	0.000	0.000	0.000	0.000	0.000
Z19 Y-2nd Trefoil	0.0051	0.0000	0.000	0.000	0.000	0.000	0.000	0.000	0.000	0.000	0.000	0.000	0.000	0.000	0.000	0.000	0.000	0.000	0.000	0.000
Z20 X-3rd Astig	0.0023	0.0000	0.000	0.000	0.000	0.000	0.000	0.000	0.000	0.000	0.000	0.000	0.000	0.000	0.000	0.000	0.000	0.000	0.000	0.000
Z21 Y-3rd Astig	0.0023	0.0000	0.000	0.000	0.000	0.000	0.000	0.000	0.000	0.000	0.000	0.000	0.000	0.000	0.000	0.000	0.000	0.000	0.000	0.000
Z22 X-3rd Coma	0.0018	0.0000	0.000	0.000	0.000	0.000	0.000	0.000	0.000	0.000	0.000	0.000	0.000	0.000	0.000	0.000	0.000	0.000	0.000	0.000
Z23 Y-3rd Coma	0.0018	0.0000	0.000	0.000	0.000	0.000	0.000	0.000	0.000	0.000	0.000	0.000	0.000	0.000	0.000	0.000	0.000	0.000	0.000	0.000
Z24 3rd Sphere	0.0018	0.0000	0.000	0.000	0.000	0.000	0.000	0.000	0.000	0.000	0.000	0.000	0.000	0.000	0.000	0.000	0.000	0.000	0.000	0.000
TOTAL		0.2609	0.000	-0.008	0.125	0.005	0.000	0.000	0.000	0.008	-0.127	-0.001	0.000	0.000	0.000	0.000	0.190	0.000	0.000	-0.001

Figure 4. Excel Spreadsheet to allocate stability amplitudes to all rigid body degrees of freedom.

It is important to note that, for the VVC-4, astigmatism sensitivity is driving the optical component rigid body alignment stability specification. Because the optical design is off-axis, Z-despace between the primary and secondary mirrors introduces both defocus and astigmatism. But, while a given despace produces 22X more defocus than astigmatism, the VVC-4 is 120X more sensitive to astigmatism than to defocus. Similarly, while the VVC-4 can accept nearly identical amounts of astigmatism, coma and trefoil, the primary mirror decenter and tilt tolerance is driven only by astigmatism – because a given PM decenter or tilt introduces 4X more astigmatism than coma and 10X more astigmatism than trefoil. Rigid body DOFs simply cannot introduce enough coma or trefoil for their sensitivities to be important. The only significant source for these WFEs are from inertial or modal bending of the primary mirror.

4. OPTICAL TELESCOPE CONCEPT

The baseline HabEx optical telescope concept is based on the HabEx-4 design concept study performed by the NASA Marshall Space Flight Center (MSFC) Advanced Concept Office (ACO) in November 2015 and published in August 2016.[9] Starting with this concept, CAD and FEM models were developed and analyzed, then iterated.

The 2015 HabEx-4 concept study was for a 4-m monolithic aperture UVOIR space observatory specifically designed for the SLS Block IB mass and volume capacities, and launch environment.[13] Its total mass was less than 11 mt (without margin). And, its structure was sized for a 3.5g axial and 1.5g lateral launch load. A ground rule for the study was that every proposed system, subsystem or component of the spacecraft (including: propulsion; attitude control; power; avionics; communication; command and data handling; etc.) should be at TRL-9 except for the primary mirror assembly, actively heater controlled straylight baffle, and science instruments. HabEx-4 was designed for a 15 year operational life at SE-L2 with no servicing. Its propellant load is sized with a 25% reserve against this 15 year operational life requirement.

HabEx-4 was a scale-up of the Exo-C 1.3-meter Mission Concept[8], with an off-axis primary mirror to provide the coronagraph with an unobscured aperture, and, science instruments on the side to both isolate them mechanically from the spacecraft and provide better thermal isolation (Figure 5 top). The primary mirror is a 200 Hz first mode, 4-meter diameter, 400 mm thick, stacked-core ULE mirror designed by the Advanced Mirror Technology Demonstrator (AMDT) project. To minimize polarization anisotropy, the Exo-C primary mirror focal length was F/2.5. Retaining this specification is what gives HabEx-4 its length. Fortunately, the SLS can accommodate this length. And, there is enough extra length for a 45 degree scarfed straylight baffle without the need for any physical deployments (Figure 5 bottom).

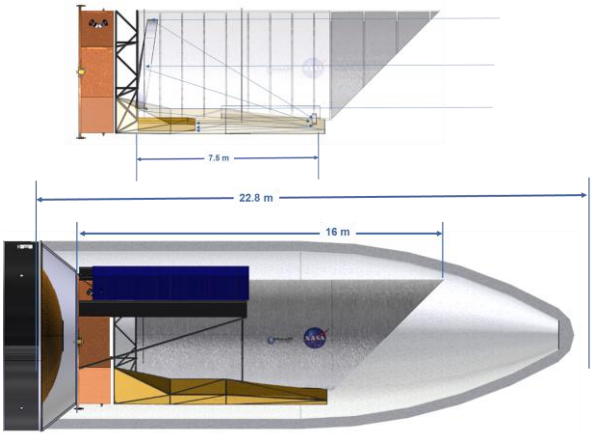

Figure 5: (top) Cutaway view of telescope; (bottom) In SLS.

The 2015 concept design was updated in 2017 by the HabEx engineering team. Given the total length of the SLS 8.4-m diameter fairing and the mass capacity of the SLS Block 1B core, a configuration considered in 2015 was to co-launch the HabEx Observatory and Star-Shade. But, definitive star-shade dimensions were not available. With 2017 mass and volume for the star-shade, it is possible to select co-launch as the baseline configuration (Figure 6). The only modification to the HabEx telescope is to make the forward scarf deployable. Figure 7 shows the baseline HabEx Observatory concept including forward scarf, actuated tube cover solar panels, sun shade and science instrument box.

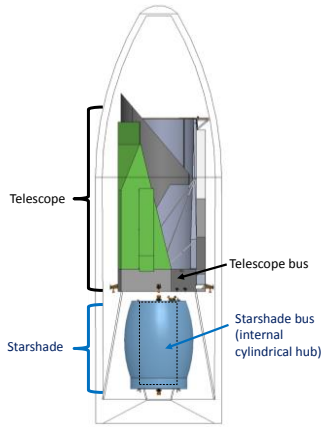

Figure 6: Co-Launch Configuration

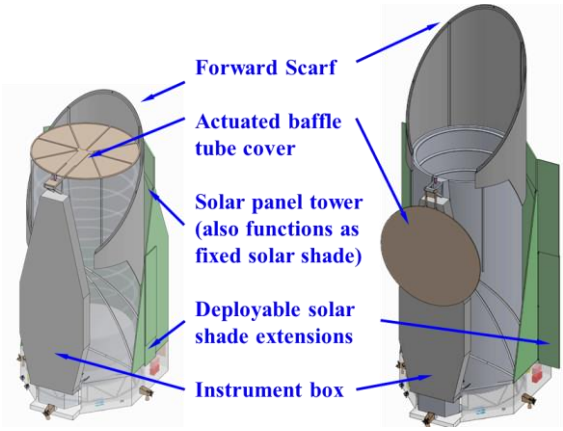

Figure 7: Observatory Concept

Figure 8 shows a FEM of the baseline HabEx 4-m off-axis telescope opto-mechanical structure used to analyze the structure's dynamic response. To maximize stiffness, the secondary mirror support tower is integral with the stray light baffle tube. The tube and its internal straylight baffles provide lateral and bending stiffness support. But, because the telescope is off-axis, the internal baffles are discontinuous. Thus, external gussets complete their support. And a 2-meter deep truss structure supports the primary mirror. The composite material for the tube and truss structure is M46J with quasi-isotopic laminate properties of 25% 0-deg, 50% 45-deg, 25% 90-deg and a density of 1.58 g/cm^3.

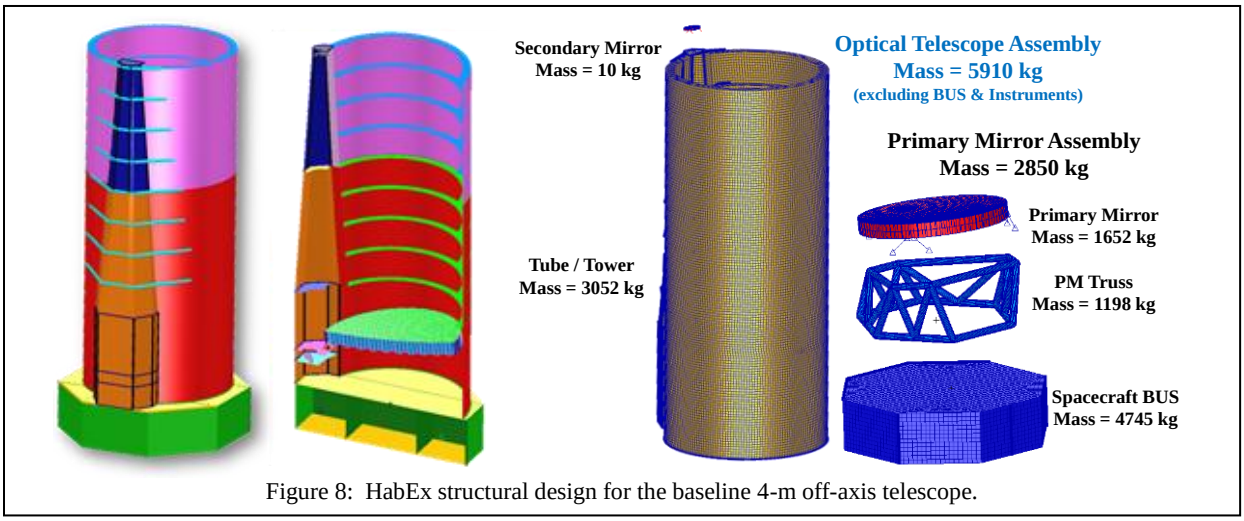

Figure 8: HabEx structural design for the baseline 4-m off-axis telescope.

5. TELESCOPE STRUCTURE DYNAMIC OPTO-MECHANICAL PERFORMANCE

The fundamental question is: Can the baseline opto-mechanical design achieve the specified rigid body stability?

To determine the telescope's dynamic response, a finite element model of the telescope and spacecraft structure was constructed and exposed to a mechanical disturbance spectrum. While HabEx is considering using low noise micro-thrusters, this analysis chose to be more conservative and assumed reaction wheels arranged on the spacecraft in a standard pyramid arrangement (Figure 9). To be even more conservative, rather than assume a specific reaction wheel, this analysis assumed the JWST enveloping specification for radial and moment disturbances (Figure 10).

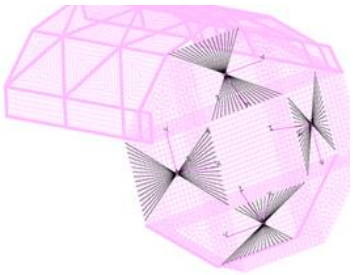

Figure 9: Pyramid Arrangement for Disturbance Spectrum Input

Figure 10: JWST Enveloping Specification for Reaction Wheel Unbalance and Vibration

The NASTRAN Multi Point Constraint (MPC) function was used to determine the rigid body displacements of the primary mirror and secondary mirror relative to the fold mirror (Figure 11). Radial force and moment disturbances were applied in 10 degree increments around wheel rotation axis; resulting in 144 load cases. Radial force and moment disturbances were swept through 360 degree wheel rotation to calculate maximum relative displacement of the mirrors relative to the reference (Figure 12) from 0 to 500 Hz. For this analysis, Critical Damping was set at 1%. It has been suggested that it be set to 0.05% for a future analysis.

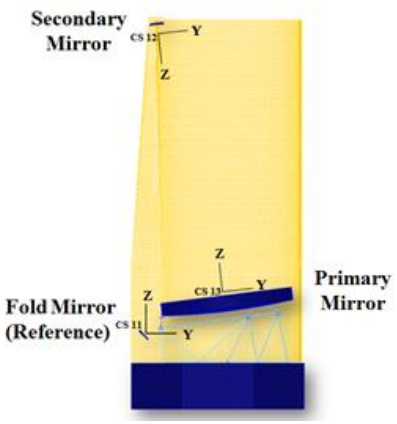

Figure 11: Mirror Displacements are relative to Fold Mirror in Coordinate System with Z-Axis normal to optical surface.

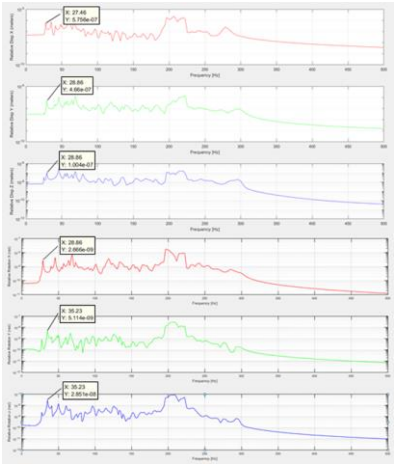

Figure 12: Maximum mirror rigid body Displacement or Rotation at each Frequency.

Table 4 lists the rigid body motion (amplitude and frequency) of the first two modes of the primary and secondary mirrors. The first mode of the primary mirror is a lateral translation (Figure 13a). The X-translation has a slightly different frequency of 27 Hz from the Y-translation at 25 Hz. The second mode of the primary mirror is a rocking or tilt mode at 40 Hz (Figure 13b). And, the first mode of the secondary mirror at 28 Hz is a lateral translation produced by a bending mode of the straylight baffle tube (Figure 14). But, without the tube, the first mode of a free standing secondary mirror would be less than 5 Hz.

Table 4: Rigid Body Motion Amplitudes of Primary Mirror and Secondary Mirror Modes			
	PM 1st Mode (translation)	PM 2nd Mode (rocking)	SM 1st Mode (tube bend)
ΔX	1.5 µm at 27 Hz	0.3 µm at 40 Hz	0.6 µm at 28 Hz
ΔY	3.6 µm at 25 Hz	0.2 µm at 40 Hz	0.5 µm at 29 Hz
ΔZ	0.6 µm at 25 Hz	1.1 µm at 40 Hz	0.1 µm at 29 Hz
ΘX	2.7 n-rad at 25 Hz	20 n-rad at 40 Hz	2.7 n-rad at 29 Hz
ΘY	9.5 n-rad at 27 Hz	26 n-rad at 40 Hz	0.8 n-rad at 28 Hz
ΘZ	6.1 n-rad at 27 Hz	1.4 n-rad at 40 Hz	24 n-rad at 28 Hz

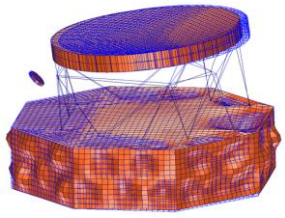

Figure 13a: Primary Mirror First Mode: 25 Hz Lateral

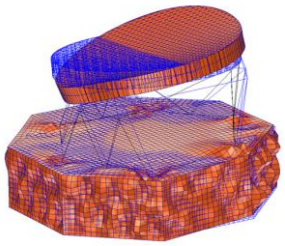

Figure 13b: Primary Mirror Second Mode: 40 Hz Tilt

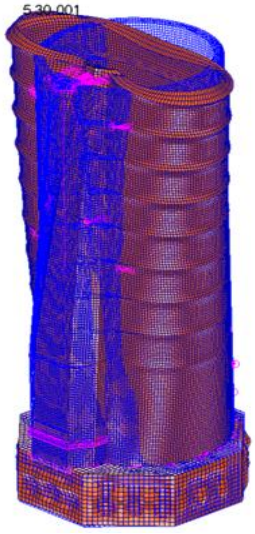

Figure 14: Secondary Mirror First Mode: 28 Hz Tube Bend

The final analysis step is to apply vibration isolation and calculate rigid body motion of the primary and secondary mirrors. Three isolation systems were analyzed: JWST Passive Isolation, Active Isolation and Micro-Thruster (Figure 15). JWST has a two stage passive isolation system. The first stage is an 8-Hz isolator between the reaction wheels and spacecraft. The second stage is a 2-Hz isolator between the spacecraft and telescope. Active isolation senses and corrects low frequency vibrations. This analysis assumes a single-stage 1-Hz active system that can attenuate low frequency vibrations by 100X (40 dB) with 15% damping.[14] For micro-thrusters, this analysis assumes a 1000X (60 dB) vibration reduction for frequencies below 2 Hz and standard mass damping for frequencies above 2 Hz.

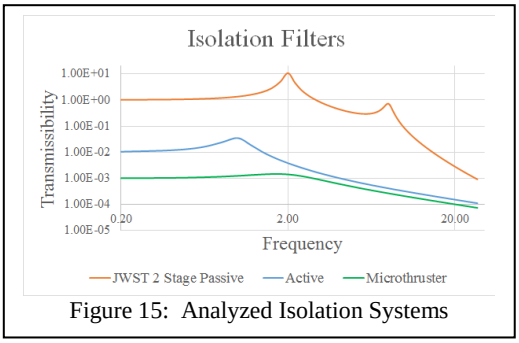

Figure 15: Analyzed Isolation Systems

Figures 16 and 17 show the amplitudes versus frequency for each rigid body degree of freedom for the Primary and Secondary Mirrors produced by the JWST Reaction Wheel Disturbance Specification and the JWST two-stage passive isolation system. Note that the amplitudes were multiplied by a 2X Model Uncertainty Factor (MUF) for frequencies below 20 Hz and a 4X MUF for frequencies above 20 Hz. The red lines are the tolerances summarized in Table 2. For this case, the HabEx baseline structure design does NOT meet the WFE stability specification for the primary mirror lateral translation modes. It does meet the specification for all higher Primary Mirror modes and all Secondary Modes.

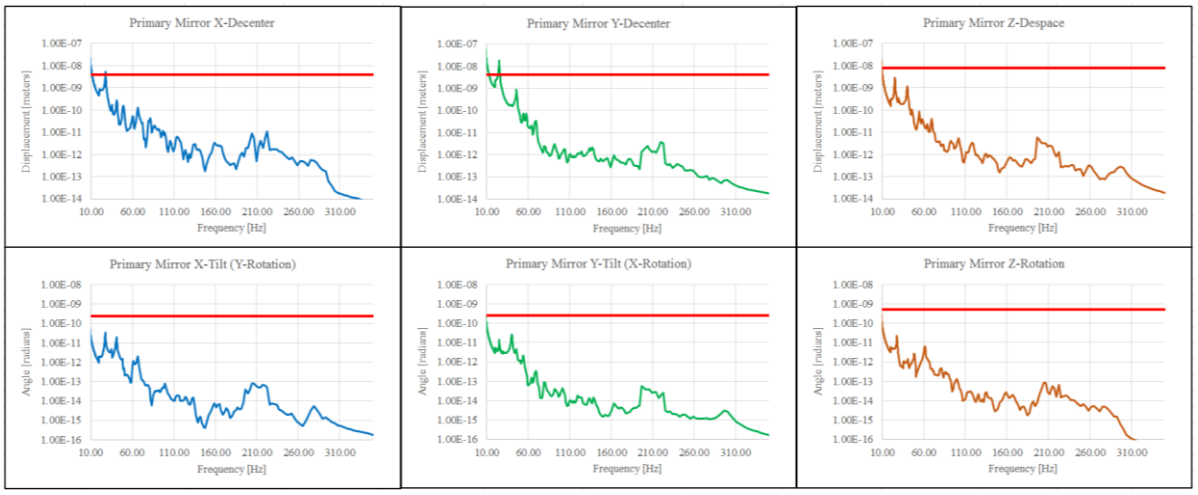

Figure 16: Primary Mirror Rigid Body Amplitudes for JWST Reaction Wheels and JWST Passive 2-Stage Isolation

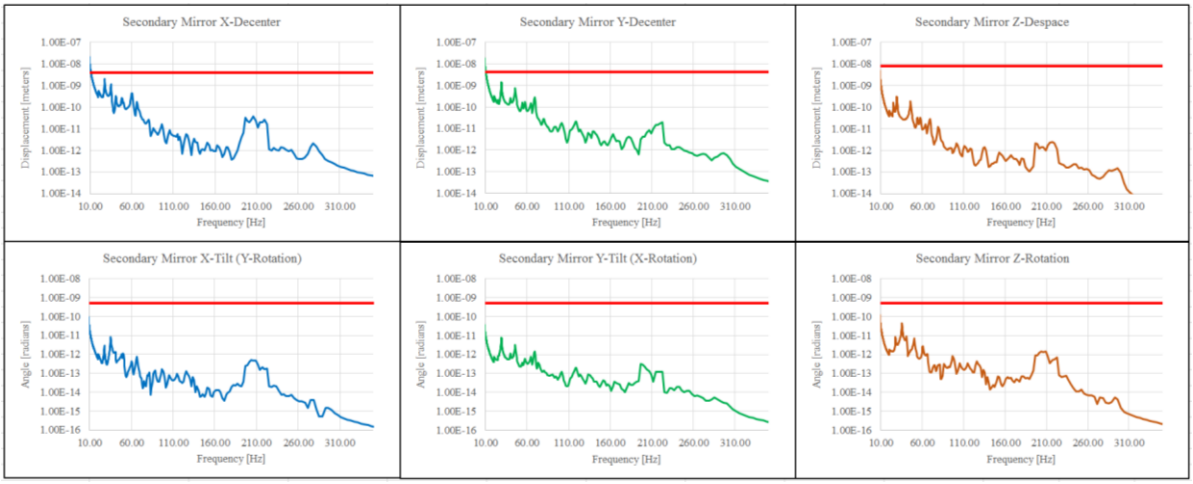

Figure 17: Secondary Mirror Rigid Body Amplitudes for JWST Reaction Wheels and JWST Passive 2-Stage Isolation

Figures 18 and 19 show the reduction in the primary mirror's rigid body motions when a 40db active isolation or a 60db micro-thrusters is assumed. As indicated by margin under the red tolerance lines, the structure design easily meets the WFE stability specification with these assumed vibration isolations.

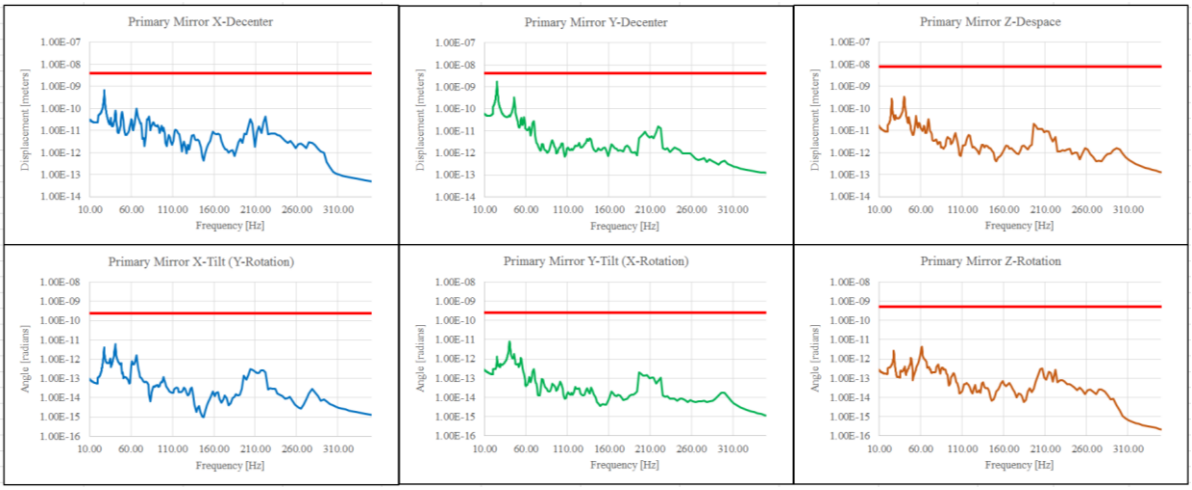

Figure 18: Primary Mirror Rigid Body Amplitudes for JWST Reaction Wheels and 40dB Active Isolation

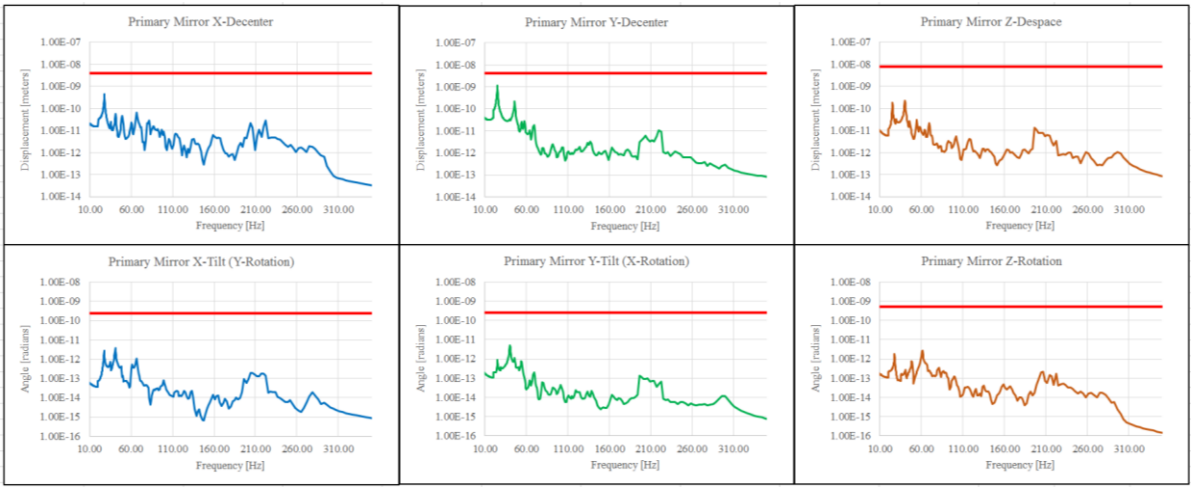

Figure 19: Secondary Mirror Rigid Body Amplitudes for JWST Reaction Wheels and 60dB Micro-Thrusters

6. CONCLUSION

The Habitable Exoplanet Imaging Mission (HabEx) is one of four missions under study for the 2020 Astrophysics Decadal Survey. Its goal is to directly image and spectroscopically characterize planetary systems in the habitable zone of Sun-like stars. Critical to achieving the HabEx science goals is a large, ultra-stable UV/Optical/Near-IR (UVOIR) telescope. The baseline HabEx telescope is a 4-meter off-axis unobscured three-mirror-anastigmatic, diffraction limited at 400 nm with wavefront stability on the order of a few 10s of picometers. The opto-mechanical design of the HabEx optical telescope assembly is a complicated, iterative systems engineering exercise that starts with system level specifications and requires experience driven intuition backed by detailed analysis. This paper has summarized the opto-mechanical design of the HabEx baseline optical telescope assembly, including a discussion of how science requirements drive the telescope's specifications, and presented an analysis of the baseline opto-mechanical design which shows that the design, using proven technology, can achieve the performance specifications necessary to perform HabEx science. The baseline 4-m off-axis HabEx opto-mechanical telescope design 'closes'.

ACKNOWLEDGEMENTS

This paper summarizes the work of the entire NASA Marshall Space Flight Center HabEx Team and our Jet Propulsion Laboratory Collaborators. MSFC Team: Michael Effinger, Scott Smith, Thomas Brooks, Jacqueline Davis, Brent Knight, Mark Stahl, Willian Arnold (AI Solution), Mike Baysinger (ESSA), Jay Garcia (ESSA), Ronald Hunt (ESSA), Andrew Singleton (ESSA), Mary Caldwell (ESSA), Melissa Therrell (ESSA), Bijan Nemati (UAH), Mary Elizabeth Cobb (UAH Intern) and Advanced Concept Office. JPL Team: Keith Warfield, Gary Juan, Stefan Martin, Stuart Shaklan, Scott Howe and Team X.

REFERENCES

[1] Committee for a Decadal Survey of Astronomy and Astrophysics; National Research Council, New Worlds, New Horizons in Astronomy and Astrophysics, The National Academies Press, Washington, D.C., 2010.
[2] NASA Space Technology Roadmaps and Priorities: Restoring NASA's Technological Edge and Paving the Way for a New Era in Space, NRC Report, 2012.
[3] Hertz, Paul, "Planning for the 2020 Decadal Survey: An Astrophysics Division White Paper", January 4, 2015, available at science.nasa.gov/astrophysics/documents/.
[4] NASA Town Hall, AAS Winter Meeting, Kissimmee, FL, 2016.
[5] Krist, Trauger, Unwin and Traub, "End-to-end coronagraphic modeling including a low-order wavefront sensor", SPIE Vol. 8422, 844253, 2012; doi: 10.1117/12.927143
[6] Harvey, James E. and Christ Ftaclas, "Diffraction effects of telescopes secondary mirror spiders on various image-quality criteria", Applied Optics, Vol. 34, No. 28, pp-6337, 1 Oct 1995.
[7] Morgan, Rhonda H., et. al., "HabEx yield modeling with for systems engineering", SPIE 10398-3, 2017.
[8] NASA, Exo-C: Imaging Nearby Worlds, CL#15-1197, March 2015
https://exep.jpl.nasa.gov/stdt/Exo-C_Final_Report_for_Unlimited_Release_150323.pdf
[9] Garreth Ruane, private communication
[10] Stuart Shaklan, private communication 10 Aug 2017
[11] Stefan Martin, private communication 10 Aug 2017
[12] Stefan Martin, private communication 18 Aug 2017
[13] Stahl, H. Philip, Randall C. Hopkins, Andrew Schnell, David Alan Smith, Angela Jackman, Keith R. Warfield, "Designing astrophysics missions for NASA's Space Launch System," J. Astron. Telesc. Instrum. Syst. 2(4), 041213 (2016), doi: 10.1117/1.JATIS.2.4.041213.
[14] Larry Dewell, Lockheed Space and Missile Systems, private communication, 4 Aug 2017